Electronic Supplementary Material (ESI) for Analytical Methods.

Supplementary information

AFM force indentation analysis on leukemia cells

*Hélène Fortier[a,b], Fabio Variola[b], Chen Wang[c] and Shan Zou[a]**

[a]Measurement Science and Standards, National Research Council of Canada, Ottawa, K1A 0R6, Canada; [b]Department of Mechanical Engineering, University of Ottawa, Ottawa, K1N 6N5, Canada; [c]Department of Pathology and Laboratory Medicine, Mount Sinai Hospital and Faculty of Medicine, University of Toronto, 600 University Avenue, Toronto, M5X 1G5, Canada.

Fitting models

Conical: $$F = \frac{2E\tan\alpha\delta^2}{\pi(1-\nu^2)}$$ Eq. S1;

Spherical: $$F = \frac{4E\sqrt{R}\delta^{3/2}}{3(1-\nu^2)}$$ Eq. S2;

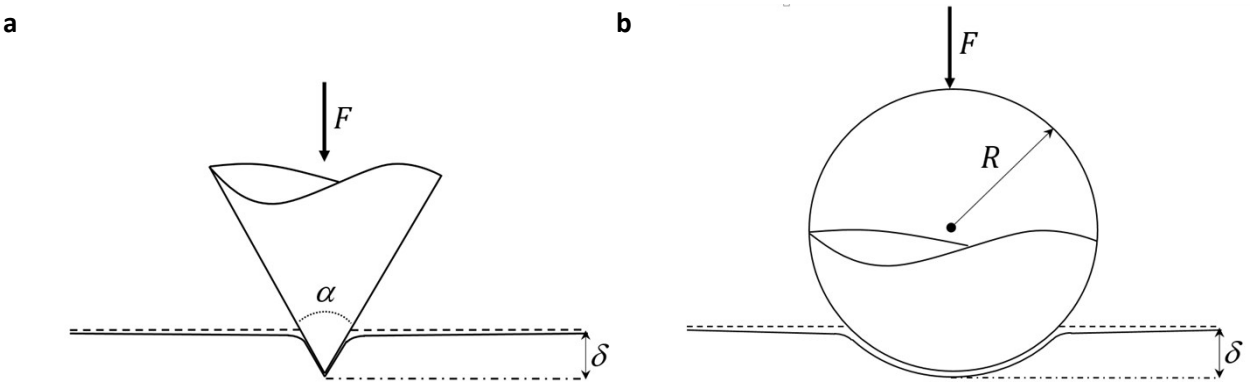

Figure S1. Contact mechanics model of a conical indenter (a) and a spherical indenter (b) both indenting an elastic half-space.

Table S1. Fitting analysis results for 49 force curves extracted consecutively using 0.5, 1.0 and 2.0 nN applied forces. Different reference points (Z_1, d_1) and (Z_2, d_2) were chosen.

Force (nN)	(Z_1, d_1) (% curve)	(Z_2, d_2) (% curve)	Average Fitting error* (nm ± SD)	Average Indentation length (nm ± SD)	Average number of data points (± SD)	Average Z_0 location (nm ± SD)
0.5	10	25	527.7 ± 204.0	1127.3 ± 379.2	1539.9 ± 558.3	-8012.8 ± 607.1
		50	477.3 ± 162.8	1011.7 ± 246.9	1367.5 ± 343.0	-7910.3 ± 527.0
		60	**454.8 ± 150.9**	**998.5 ± 257.8**	**1349.9 ± 360.2**	**-7897.2 ± 515.1**
		75	442.8 ± 148.9	973.4 ± 259.3	1314.9 ± 361.2	-7872.0 ± 511.0
		90	431.8 ± 140.3	955.5 ± 237.6	1288.8 ± 327.5	-7854.1 ± 501.8
	15	25	497.5 ± 230.8	1102.7 ± 397.4	1508.9 ± 593.9	-7963.2 ± 607.5
		50	449.5 ± 163.7	989.3 ± 271.1	1337.1 ± 378.6	-7887.9 ± 523.6
		60	429.9 ± 151.1	975.5 ± 267.9	1318.8 ± 376.5	-7874.1 ± 492.2
		75	418.7 ± 157.5	934.6 ± 267.5	1261.3 ± 373.1	-7833.0 ± 499.6
		90	404.3 ± 143.0	909.5 ± 243.6	1225.3 ± 335.8	-7808.0 ± 500.0
1.0	10	25	508.6 ± 207.1	1067.3 ± 372.9	1496.6 ± 548.6	-5424.7 ± 796.8
		50	432.8 ± 169.7	913.1 ± 286.6	1265.6 ± 379.7	-5269.9 ± 816.8
		60	412.0 ± 164.8	893.8 ± 290.3	1237.8 ± 382.3	-5250.6 ± 832.1
		75	390.9 ± 167.0	858.0 ± 282.0	1184.4 ± 353.5	-5214.7 ± 852.3
		90	390.5 ± 178.0	864.7 ± 304.0	1194.2 ± 387.1	-5221.4 ± 874.5
	15	25	472.4 ± 197.5	992.1 ± 350.3	1384.1 ± 497.8	-5349.2 ± 815.4
		50	405.4 ± 180.9	885.5 ± 315.2	1224.4 ± 406.8	-5242.2 ± 862.2
		60	372.0 ± 180.9	841.9 ± 311.6	1162.3 ± 401.4	-5198.4 ± 877.3
		75	369.1 ± 188.1	824.3 ± 314.9	1136.8 ± 402.2	-5180.6 ± 879.2
		90	174.5 ± 70.0	819.2 ± 332.0	1128.7 ± 420.5	-5175.5 ± 907.5
2.0	10	25	443.8 ± 127.8	935.7 ± 226.8	1337.0 ± 336.9	-5191.1 ± 390.4
		50	416.9 ± 86.2	889.9 ± 143.1	1268.2 ± 199.4	-5145.1 ± 357.9
		60	409.8 ± 83.3	884.5 ± 135.7	1260.4 ± 189.0	-5139.6 ± 354.4
		75	401.6 ± 77.7	871.8 ± 133.6	1242.1 ± 185.7	-5126.8 ± 358.2
		90	396.2 ± 68.5	870.1 ± 126.7	1239.6 ± 175.3	-5125.1 ± 347.7
	15	25	431.3 ± 113.9	903.9 ± 172.5	1288.0 ± 239.4	-5159.0 ± 383.1
		50	406.8 ± 94.5	875.4 ± 149.8	1246.4 ± 203.3	-5130.3 ± 362.9
		60	399.3 ± 88.5	872.6 ± 140.0	1242.4 ± 188.5	-5127.6 ± 356.3
		75	392.9 ± 77.5	861.6 ± 132.9	1226.7 ± 179.5	-5116.4 ± 352.1
		90	385.4 ± 71.2	855.4 ± 129.5	1217.9 ± 175.8	-5110.2 ± 348.2

*Fitting error = $\sqrt{\frac{\sum\left(d_{data_i} - d_{model_i}\right)^2}{n}}$ Eq. S3;

Table S2. Fitting analysis results for 49 force curves extracted consecutively using a 1.0 nN applied force. Different reference points (Z_1, d_1) and (Z_2, d_2) were chosen. All results are compared to the reference at which (Z_1, d_1) and (Z_2, d_2) are set at 10% and 60%, respectively.

(Z_1, d_1) (% curve)	(Z_2, d_2) (% curve)	Average variation ratio of the fitting error* ($\pm$ C_v)	Average variation ratio of the indentation length* ($\pm$ C_v)	Average variation ratio of the number of data points* ($\pm$ C_v)	Average variation ratio of the Z_0 location* ($\pm$ C_v)
	25	1.23 ± 0.41	1.19 ± 0.35	1.21 ± 0.37	1.03 ± 0.15
	50	1.05 ± 0.39	1.02 ± 0.31	1.02 ± 0.30	1.00 ± 0.15
10	**60**	**1.00 ± 0.40**	**1.00 ± 0.32**	**1.00 ± 0.31**	**1.00 ± 0.16**
	75	0.95 ± 0.43	0.96 ± 0.33	0.96 ± 0.30	0.99 ± 0.16
	90	0.95 ± 0.46	0.97 ± 0.35	0.96 ± 0.32	0.99 ± 0.17
	25	1.15 ± 0.42	1.11 ± 0.35	1.12 ± 0.36	1.02 ± 0.15
	50	0.98 ± 0.45	0.99 ± 0.36	0.99 ± 0.33	1.00 ± 0.16
15	60	0.90 ± 0.49	0.94 ± 0.37	0.94 ± 0.35	0.99 ± 0.17
	75	0.90 ± 0.51	0.92 ± 0.38	0.92 ± 0.35	0.99 ± 0.17
	90	0.42 ± 0.40	0.92 ± 0.41	0.91 ± 0.37	0.99 ± 0.18

Table S3. Fitting analysis results for 49 force curves extracted consecutively using 2.0 nN applied force. Different reference points (Z_1, d_1) and (Z_2, d_2) were chosen. All results are compared to the reference at which (Z_1, d_1) and (Z_2, d_2) are set at 10% and 60%, respectively.

(Z_1, d_1) (% curve)	(Z_2, d_2) (% curve)	Average variation ratio of the fitting error* (± C_v)	Average variation ratio of the indentation length* (± C_v)	Average variation ratio of the number of data points* (± C_v)	Average variation ratio of the Z_0 location* (± C_v)
	25	1.08 ± 0.29	1.06 ± 0.24	1.06 ± 0.25	1.01 ± 0.08
	50	1.02 ± 0.21	1.01 ± 0.16	1.01 ± 0.16	1.00 ± 0.07
10	**60**	**1.00 ± 0.20**	**1.00 ± 0.15**	**1.00 ± 0.15**	**1.00 ± 0.07**
	75	0.98 ± 0.19	0.99 ± 0.15	0.99 ± 0.15	1.00 ± 0.07
	90	0.97 ± 0.17	0.98 ± 0.15	0.98 ± 0.14	1.00 ± 0.07
	25	1.05 ± 0.26	1.02 ± 0.19	1.02 ± 0.19	1.00 ± 0.07
	50	0.99 ± 0.23	0.99 ± 0.17	0.99 ± 0.16	1.00 ± 0.07
15	60	0.97 ± 0.22	0.99 ± 0.16	0.99 ± 0.15	1.00 ± 0.07
	75	0.96 ± 0.20	0.97 ± 0.15	0.97 ± 0.15	1.00 ± 0.07
	90	0.94 ± 0.18	0.97 ± 0.15	0.97 ± 0.14	0.99 ± 0.07

Coefficient of Variation $= C_v = \left({SD}/{\bar{x}}\right)$ Eq. S4 ;

Mean $= \bar{x} = \frac{1}{n}\sum_{i=0}^{n} x_i$ Eq. S5 ;

Table S4. Elasticity measurements on 5 different NB4 cells for each assessed force applied of 0.5 nN, 1.0 nN and 2.0 nN, respectively, using both a spherical probe and a conical one. Young's modulus values were obtained by fitting 49 deflection-displacement curves to the respective models.

Force (nN)	Model	Cell (% curve)	Minimum Young's Modulus (kPa)	Maximum Young's Modulus (kPa)	Average Young's Modulus (kPa ± SD)	Overall average of the Young's Modulus (kPa ± SD)
0.5	Spherical	1	0.038	0.304	0.104 ± 0.052	**0.159 ± 0.066**
		2	0.023	0.094	0.055 ± 0.017	
		3	0.082	0.581	0.295 ± 0.097	
		4	0.030	0.398	0.161 ± 0.099	
		5	0.038	0.328	0.180 ± 0.067	
	Conical	A	0.109	1.031	0.582 ± 0.202	**0.697 ± 0.339**
		B	0.267	2.123	0.771 ± 0.386	
		C	0.178	0.627	0.361 ± 0.125	
		D	0.142	3.002	1.166 ± 0.796	
		E	0.247	1.079	0.603 ± 0.186	
1.0	Spherical	6	0.065	0.601	0.228 ± 0.100	**0.222 ± 0.082**
		7	0.097	0.278	0.185 ± 0.043	
		8	0.181	0.617	0.281 ± 0.090	
		9	0.072	0.709	0.237 ± 0.137	
		10	0.062	0.251	0.178 ± 0.039	
	Conical	F	0.383	1.723	0.643 ± 0.208	**0.874 ± 0.249**
		G	0.388	1.245	0.863 ± 0.231	
		H	0.443	2.096	0.582 ± 0.244	
		I	0.895	2.682	1.563 ± 0.396	
		J	0.411	1.123	0.716 ± 0.167	
2.0	Spherical	11	0.244	0.740	0.462 ± 0.105	**0.335 ± 0.063**
		12	0.131	0.226	0.170 ± 0.020	
		13	0.294	0.679	0.498 ± 0.107	
		14	0.123	0.415	0.323 ± 0.049	
		15	0.138	0.316	0.222 ± 0.036	
	Conical	K	0.647	1.725	1.314 ± 0.211	**1.088 ± 0.222**
		L	0.792	1.903	1.441 ± 0.226	
		M	0.042	0.064	0.049 ± 0.005	
		N	0.815	3.410	2.009 ± 0.570	
		O	0.459	0.867	0.626 ± 0.095	

Table S5. Young's modulus dependency of the fitted indentation length of 49 force curves extracted consecutively over a single NB4 cell using an applied load of 0.5 nN and spherical probe and model.

Defined indentation length (nm)	Measured Indentation length (nm ± SD)	Minimum Indentation length (nm)	Maximum Indentation length (nm)	Average Young's Modulus (kPa ± SD)	Minimum Young's Modulus (kPa)	Maximum Young's Modulus (kPa)
200	199.94 ± 0.32	198.89	200.61	0.164 ± 0.106	0.077	0.677
400	399.83 ± 0.27	399.29	400.55	0.110 ± 0.059	0.029	0.325
600	596.36 ± 16.88	488.19	600.64	0.103 ± 0.054	0.020	0.304
800	766.04 ± 76.49	488.19	800.74	0.103 ± 0.053	0.023	0.304
1000	892.80 ± 148.71	488.19	1000.45	0.103 ± 0.053	0.030	0.304
Whole curve	998.54 ± 257.76	488.19	1612.69	0.104 ± 0.052	0.040	0.304

Automated Data Processing Code

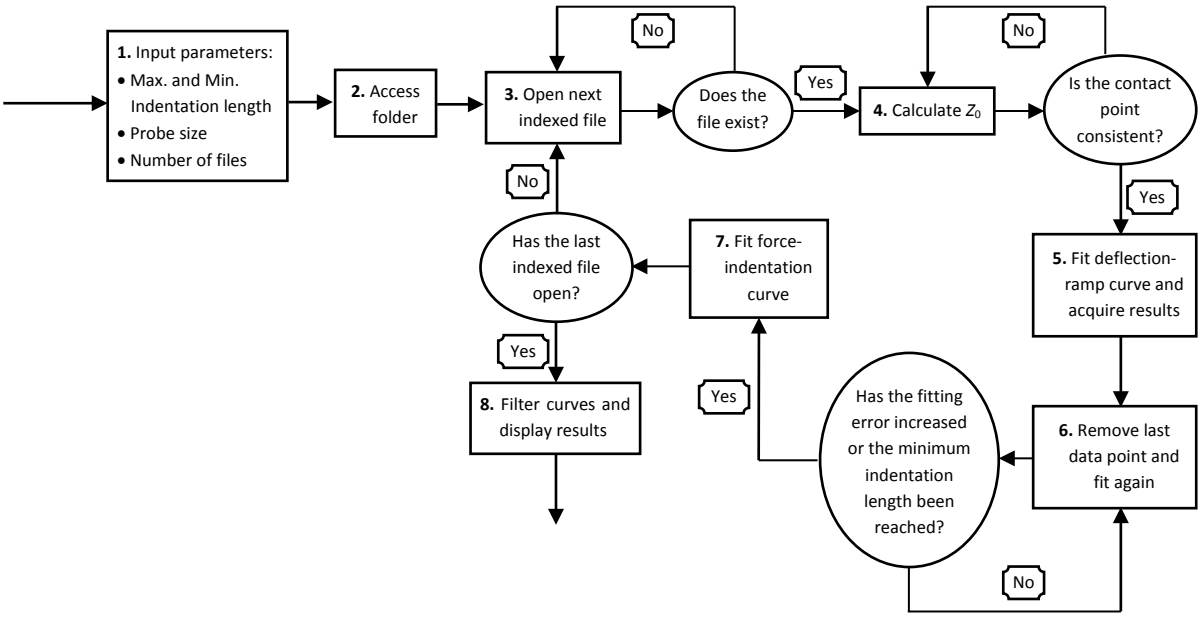

Figure S2. The design of the analysis code processing steps, including the input of fitting parameters (1), accessing folder (2), opening indexed file (3), calculating the contact point (4), fitting the deflection-ramp curve (5) minimizing the fitting error (6), fitting the force-indentation curve (7), and filtering and displaying results (8).

As illustrated in Figure S2, the first step requires the user to indicate specific physical and geometrical parameters (*i.e.* spring constant (k), Poisson ratio (ν) and probe size (R or α)) in addition to other variables such as the number of force curves, the folder path location and the file name. Once launched, the first indexed ASCII file (or curve) retrieved from a specific folder (step 2) is opened: the deflection and ramp waves of a single force curve are now loaded (Figure S2, step 3). Successively, an initial approximation of the contact point location is set according to the profile of the curve (*i.e.*, close to the non-linear portion). Based on Eq. 3 and Eq. 4, the calculations of the Z_0 are repeated until the location values from consecutive processes remain the same. The corresponding d_0 should now be offset to zero (Figure S2, step 4). The following step is to fit the deflection-ramp curve once using the maximum or portion of the indentation length (Figure S2, step 5), a parameter provided by the user, using the least squares method. The curve is fit again by deleting the last data point, and the code will stop processing until the fitting error does not increase or the minimum indentation length is

reached (Figure S2, step 6). The fitting information and fit results such as the Young's modulus (calculated by using both a deflection-ramp curve and a force-indentation curve), fitting errors, number of fitted data points and contact point location, as well as the specific curve numbers is recorded and tracked (*i.e.*, each deflection curve is numbered and fitting information for each of them is linked to that number). From this accessible fitting information, specific fitting criteria were defined, such as the reference points that should be used to locate the contact point. Furthermore, the force-indentation curve is also fit as additional evidence of the data compliance with the model (Figure S2, step 7). Finally, the code returns to step 3 and repeats the procedure using the next indexed file.

When collecting a force map with the AFM, a force set folder is saved including the indexed deflection-ramp distance curves as text files. Thus, when the code consecutively investigates each text file, it stops once the last indexed file within a recorded force set is processed. When the fitting criteria are not met some of the curves including no tip-sample contact, incomplete curves (*i.e.*, with smaller scan lengths or applied forces than the experimental settings), and curves with an insufficient amount of data points can be filtered by the code. This option enables fast analysis of the average fitting information (see Batch analysis code performance section for further details). It can also plot histograms to observe the full data set and their variability (Figure S2, step 8).

The automated batch analysis algorithm has a unique looping protocol for Young's modulus extraction from individual curves as it thoroughly analyzes each one of them and focuses on the importance of systematic assessment and not on average results. Programming was also created to be user-friendly. In particular, users are assisted step by step throughout their fitting process.

Batch analysis code performance

Code options

In order to automatically process a large number of force curves, the analysis code was developed involving different fitting options (*vide supra*), such as contact point criteria, the use

of the spherical or conical model to fit either the approaching or retracting force curves, as well as manual parameter inputs such as the Poisson ratio and spring constant. These options are fully controllable and functional for comparing the fitting results.

The first option in the code is to manually change the fitting parameters such as the Poisson ratio (υ), spherical probe radius (*R*) or conical probe opening angle (α) and spring constant (*k*) of the cantilever. Easy access to these parameters helps in identifying the impact of each of these parameters on the fitting themselves. Additionally, it is possible to observe the fit curve overlaying the raw data if required by the user. This is often considered and needed when the calculated fitting errors are larger than expected for some particular curves. It allows a quick overview of the force curve batch as the fittings are performed. Of course, both conical and spherical fitting models were introduced in the batch analysis code to compare the variability of the data and elasticity measurements using either of them.

Code options involve the choice of using either the retracting or the approaching force curve for the fitting. The curve itself can also be fit within an indentation range which may be specified by the user. By selecting different minimum and maximum indentation length to fit the force curves, it is possible to determine the softer and harder indentation regimes of a deflection curve.

As deflection-displacement measurements are performed within a dynamic system, curves must be tracked thoroughly to avoid measuring neighboring cell motion, or cantilever resonance. In order to efficiently assess the affected force curves, specific filtering criteria are required. For fast analysis purposes and to obtain a meaningful value for the average data output, force curves can also be filtered to identify outliers which often include force curves that are inconsistent with the fitting model. The most accurate way to identify these curves is to compare the Young's modulus given by the deflection-*z*-piezo displacement curve with the one extracted from the force-indentation curve. Ideal curves that comply with the model promise to generate the same Young's modulus values using either model. This criterion was chosen as it applies to any sample and fitting model used, meanwhile fitting errors can vary according to the number of data points within a force curve.

Moreover, consistency in identifying the contact point of the deflection *vs. z*-piezo displacement curves using two data points (Z_1, d_1) and (Z_2, d_2) for calculation was found to be a good indicator for sorting the curves. In the case of APL-NB4 cells, curves that have a contact point differing of over 500 nm when calculated using different (Z_1, d_1) and (Z_2, d_2) reference points should be considered as outliers. Finally, curves that were missing a baseline to properly measure the contact point were considered to not conform to the fitting models and were filtered out.

Batch analysis efficiency

As manually fitting a force curve may take over 10 min when calculating and recalculating the contact point before extracting the Young's modulus, a fast and reliable batch analysis code was required. Data collection time alone is dependent on AFM parameters used, such as the force map grid size, sample rate, and delays (or dwell time) of approach and retract.

Table S6. Time efficiency of the batch analysis code.

Force map grid size	**7 x 7, n=49**	**15 x 15, n=225**	**25 x 25, n = 625**	**64 x 64, n=4096**
Exporting Map to ACSII file time (h:min:s)	~ 0:0:45	~ 0:0:45	~ 0:0:45	~ 0:0:45
File loading time (h:min:s)	~ 0:0:50	~ 0:0:50	~ 0:0:50	~ 0:0:50
Fitting time (h:min:s)	~ 0:0:16	~ 0:1:15	~ 0:3:47	~ 0:55:36
Total time (h:min:s)	~ 0:1:51	~ 0:2:50	~ 0:5:22	~ 0:57:11

*Sample rate : 2047 Hz

Table shows the time efficiency of the batch analysis code for different force map grids evaluated using a 2.40 Hz processor. Time required exporting the collected force map as ACSII files and loading them in the IGOR Pro software are mostly dependent on the speed of users. However, fitting time is related to the number of curves to be fit. Hence, data processing is more efficient when a greater number of curves, n, is processed. Unfortunately, the code may only fit a single force map at a time. Thus, between each force map, file path must be located

and the specified fitting model and its parameters must be selected before loading the curves. These aspects will be part of further improvement of the code itself.